Compact, fiber-compatible, cascaded Raman laser

Bumki Min, Tobias J. Kippenberg, and Kerry J. Vahala

Department of Applied Physics, California Institute of Technology, Pasadena, California 91125

Received April 23, 2003

Cascaded Raman Stokes lasing in an ultrahigh-Q silica microsphere resonator coupled to a tapered fiber is demonstrated and analyzed. With less than 900 μW of pump power near 980 nm, five cascaded Stokes lasing lines are generated. In addition, a threshold power of 56.4 μW for the first-order Stokes lasing is achieved. The Stokes lasing lines exhibit distinct characteristics depending on their order, as predicted by theoretical analysis. © 2003 Optical Society of America

OCIS codes: 140.3550, 140.4780, 190.5650, 230.3990.

Cascaded Raman lasers have been of considerable interest as a means of extending the wavelength range of existing laser sources. Demonstrations of cascaded Raman (Stokes) lasing in both fiber-based Bragg grating resonator[1] media and bulk-crystal active media[2] embedded in a Fabry–Perot resonator have been realized. Recently, a microcavity-based Raman laser with an ultrahigh-Q silica microsphere was demonstrated.[3] In addition to being both compact and efficient, this device features pump and signal coupling directly to optical fiber, a significant advantage in practical applications. In this Letter we report the first observation to our knowledge of cascaded operation in these devices, which can achieve as high as fifth-order Raman lasing with submilliwatt pump powers. To our knowledge these devices are both the smallest fiber-compatible cascade devices ever reported and the most efficient in terms of their threshold, exhibiting threshold powers that are more than 2 orders of magnitude lower than those of cascaded operation of Raman lasers based on fiber Bragg gratings.[1]

The whispering-gallery modes (WGMs) of microspheres fabricated from fused silica have achieved one of the highest Q factors (8×10^9) to date.[4] The ultrahigh Q combined with the small mode volume ($\sim$1000 μm^3 in this work) allow resonant buildup of very high circulating intensities, thereby significantly reducing the threshold for stimulated nonlinear processes. These properties of high-Q WGMs were first demonstrated in the pioneering work of Qian and Chang[5] and Lin and Campillo[6] concerning nonlinearities in microdroplets, including the observation of Raman cascading as high as 14th order.[5] However, the required pump power in these experiments was large (typically several watts) owing to inefficient modal excitation provided by free-space illumination. Modal excitation with fiber tapers, on the other hand, allows excitation of a single WGM with ultralow coupling loss,[7] thereby drastically improving the overall efficiency while providing convenient access to the technologically important fiber-transport medium. As demonstrated here, the use of tapered optical fibers also allows precise measurements on the higher-order Stokes waves.

The microsphere resonator modes are modeled as coupled harmonic oscillators with external input field and nonlinear Raman terms[8–11]:

$$\frac{da_0}{dt} = -\frac{1}{2\tau_0}\, a_0 + \kappa_0 s - \frac{\omega_0}{\omega_1}\, g_1 a_0 |a_1|^2, \tag{1}$$

$$\frac{da_j}{dt} = -\frac{1}{2\tau_j}\, a_j + g_j a_j |a_{j-1}|^2 - \frac{\omega_j}{\omega_{j+1}}\, g_{j+1} a_j |a_{j+1}|^2, \quad (j = 1, 2, \ldots, N-1), \tag{2}$$

$$\frac{da_N}{dt} = -\frac{1}{2\tau_N}\, a_N + g_N a_N |a_{N-1}|^2, \tag{3}$$

where a_j is the slowly varying cavity field amplitude of the jth Stokes wave; τ_j and g_j are the corresponding photon lifetime[9,10] and intracavity Raman gain coefficient (proportional to the bulk Raman gain coefficient g_R^B),[3,12] respectively; s is the input pump field amplitude ($|s|^2 = P_{\text{in}}$, the input pump power); and κ_j is the coupling coefficient.[9] In a steady state, recursion relations are obtained where the initial starting term is taken as the $(N-1)$th clamped intracavity Stokes energy. With these recursion relations the intracavity Stokes energies of all orders in the microsphere can be solved iteratively. The even- and odd-order (highest) Stokes output powers are given by the following expressions, where the parameter α_j is introduced for simplicity [defined by $\alpha_j \equiv 1/(2\tau_j)$]:

$$P_N \equiv |\kappa_N|^2 |a_N|^2 = \frac{|\kappa_0|^2 |\kappa_N|^2}{g_0{}^2 \left(\sum_{k=0}^{N/2} \frac{\alpha_{N-2k}}{g_{N-2k}} \right)} P_{\text{in}} - |\kappa_N|^2 \sum_{k=1}^{N/2} \frac{\alpha_{N-(2k-1)}}{g_{N-(2k-1)}} \quad (N \text{ even}), \tag{4}$$

$$P_N \equiv |\kappa_N|^2 |a_N|^2 = \frac{|\kappa_0|\,|\kappa_N|^2}{g_0 \left[\sum_{k=0}^{(N-1)/2} \frac{\alpha_{N-2k}}{g_{N-2k}} \right]^{1/2}} \sqrt{P_{\text{in}}} - |\kappa_N|^2 \sum_{k=1}^{(N+1)/2} \frac{\alpha_{N-(2k-1)}}{g_{N-(2k-1)}} \quad (N \text{ odd}). \tag{5}$$

These equations show that the even-numbered, highest-order, Stokes lasing power increases linearly

0146-9592/03/171507-03$15.00/0

with the input pump power, whereas for the odd-numbered case power increases in proportion to the square root of the input pump power. Analysis also shows that for an odd number of Stokes lasing lines all of the even-numbered Stokes lines are clamped and vice versa.

From the relation between g_j and $g_R{}^B$, the threshold pump powers for the highest-order Stokes lasing lines can be derived as follows[12]:

$$P_{\mathrm{th}} = \frac{\pi^2 n^2}{\lambda_0 \lambda_1} \frac{V_{\mathrm{eff}}}{g_R{}^B} \left(\sum_{k=0}^{N/2} \frac{1}{Q_{t,N-2k}} \right)^2 \times \sum_{k=1}^{N/2} \frac{Q_{e,0}}{Q_{t,N-(2k-1)}} \qquad (N \text{ even}), \tag{6}$$

$$P_{\mathrm{th}} = \frac{\pi^2 n^2}{\lambda_0 \lambda_1} \frac{V_{\mathrm{eff}}}{g_R{}^B} \left(\sum_{k=1}^{(N+1)/2} \frac{1}{Q_{t,N-(2k-1)}} \right)^2 \times \sum_{k=0}^{(N-1)/2} \frac{Q_{e,0}}{Q_{t,N-2k}} \qquad (N \text{ odd}), \tag{7}$$

where n is the refractive index of the microsphere, $Q_{e,0}$ is the external quality factor at the pump wavelength, and $Q_{t,j}$ is the loaded quality factor at the jth Stokes wavelength.

Figure 1 shows a typical spectrum of a microsphere cascaded Raman Stokes laser excited by a tunable, narrow-linewidth (<300 kHz), external-cavity laser near the wavelength of 980 nm. The output Stokes lasing was highly multimode because of the large Raman gain bandwidth and the small free spectral range of the microspheres involved in this study. To characterize the conversion of power from the pump mode to the higher-order Stokes lines, the peak output Stokes power was measured while the high-Q resonance at the pump wavelength was repeatedly scanned with a function generator. The microspheres tested ranged in diameter from 50 to 60 μm, and a fiber taper with a waist diameter of 1–2 μm was used for excitation of the fundamental $l = m$ and near-fundamental WGMs. The loaded Q factor at the pump wavelength was estimated to be in the range 10^7–10^8 as determined by linewidth measurement. The inset in Fig. 1 is a micrograph showing the microsphere tapered-fiber system. Figure 2(a) is a theoretical plot of cascade output powers versus pump power based on Eqs. (4) and (5). Here the pump wavelength is 980 nm; the intrinsic Q factors for each Stokes wavelength are assumed to be 1.5×10^8; the microsphere and the fiber taper diameters are 60 μm and 1 μm, respectively; and the gap distance between the microsphere and the fiber taper is set to the critical coupling point (0.253 μm) at the pump wavelength. The external Q factors were calculated according to the formula given in Ref. 8. Figure 2(b) shows the measured output versus input power relations as high as fourth order. Each data set was taken when the order presented was the highest order in the spectrum. The data exhibit the theoretically predicted behavior that odd-numbered lines increase proportional to the square root of the input pump power, whereas even-numbered lines vary linearly with the input pump power [corresponding regions in Fig. 2(a) are indicated for comparison]. Figure 2(b) (upper left panel) also shows the clamped response for the onset of a next-order Stokes laser line. As a general comment, quantum efficiencies in these data sets were made intentionally low (and thresholds high) by operation in the undercoupled regime. This enabled more consistent data collection because small

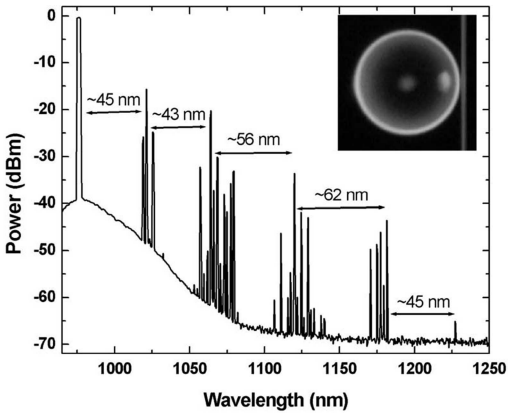

Fig. 1. Typical emission spectrum of the microsphere cascaded Raman laser. The pump wavelength is at 976.08 nm. Inset: optical micrograph of a microsphere taper system used in the experiment.

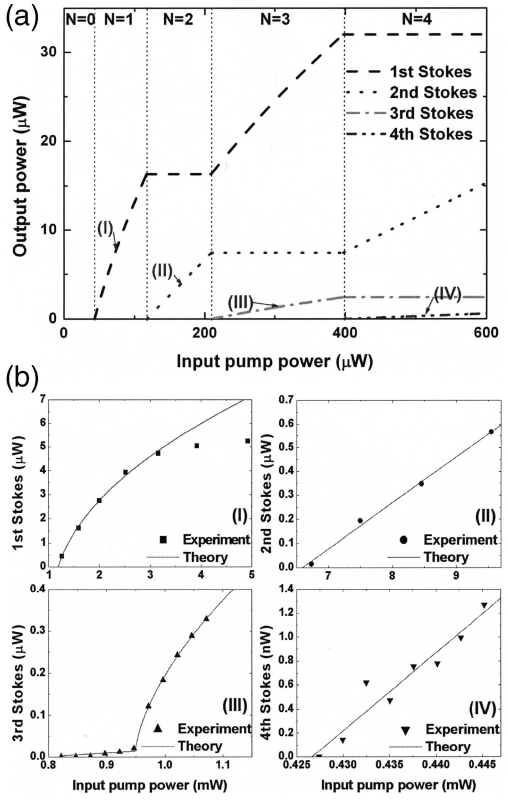

Fig. 2. (a) Theoretical plot of output Raman Stokes power as high as fourth order. (b) Stokes lasing powers (first, second, 1550-nm pumping; third, fourth, 980-nm pumping) versus input pump power. Each data set corresponds to measurements taken with a different sphere.

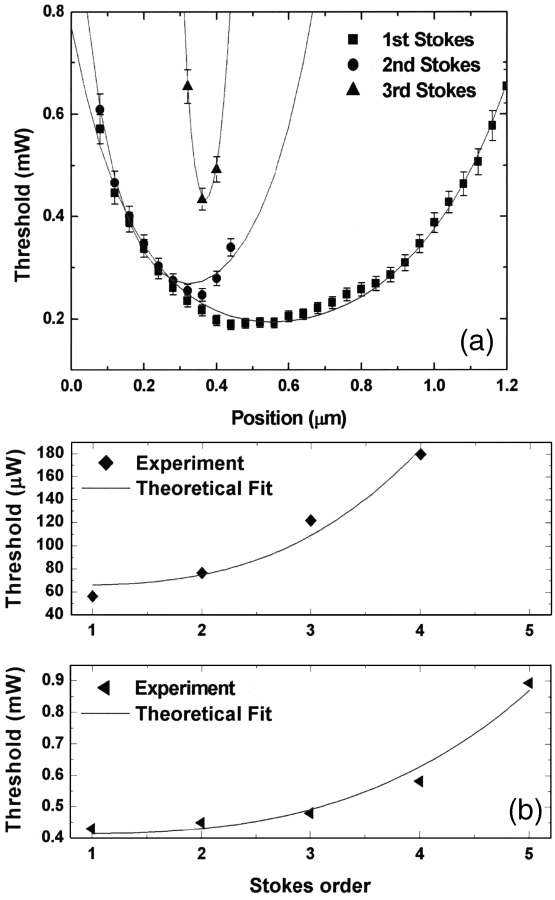

Fig. 3. (a) Threshold pump power versus the gap distance for various Stokes orders (sphere–taper contact location was set at 0 μm). (b) Threshold pump power versus Stokes order and theoretical curve (solid curve) for two different spheres.

changes in the taper–sphere gap induce a less abrupt power variation in the undercoupled regime than in the overcoupled regime. In addition, multimode operation of the microsphere laser, particularly at the shorter pump wavelength, reduced single-line quantum efficiency further. A differential quantum efficiency (unidirectional) of 6.48% was observed for first-order Stokes lasing with 980-nm-band pumping. Figure 3(a) shows the measured threshold pump power versus the taper–sphere gap distance for several Stokes lines. A single sphere was used for all measurements, and the gap distance was controlled by a piezomotor with a step size of 20 nm. The observed dependence of the minimum-threshold gap on the Stokes order is attributed to a dependence of Q_e and Q_0 on wavelength. The external quality factor Q_e is dependent on the wavelength through the phase-matching condition. (In the experiment the fiber diameter was controlled to achieve effective phase match at the pump wavelength.) The theoretical fit is made by assuming the external Q factor is in the form of an exponential function of the gap distance.[8]

The two plots in Fig. 3(b) show the measured threshold dependence on the Stokes order for two different microspheres (each plot was taken with a single sphere). In this measurement the loading conditions were optimized for each data point by adjusting the taper–sphere gap. The asymptotic threshold pump power dependence on the Stokes order (as the Stokes order increases) can be inferred from Eqs. (6) and (7) to be a cubic function of the Stokes order, assuming all the loaded Q factors are the same at each wavelength. The experimental results in Fig. 3(b) confirm this cubic dependence; in addition, one point in these data exhibited a record-low threshold pump power of 56.4 μW for onset of first-order Stokes lasing [upper panel in Fig. 3(b)]. Furthermore, the data show a record threshold for cascaded operation more than 2 orders of magnitude lower than for fiber Raman cascaded lasers.[1]

In conclusion, we have demonstrated cascaded Raman lasing in an ultrahigh-Q microsphere coupled to a tapered optical fiber. Raman Stokes lasing as high as fifth order was observed with submilliwatt pump power. The threshold power for first-order Raman lasing was as low as 56.4 μW. Even- and odd-numbered Raman lasing lines exhibited different output power versus input pump power relations in agreement with theory. The threshold power was observed to follow an approximately cubic dependence on the order, as predicted by theory.

This work was supported by the Defense Advanced Research Project Agency, the National Science Foundation, and the Caltech Lee Center. The authors thank L. Yang for helpful discussion. K. J. Vahala's e-mail address is vahala@caltech.edu.

References

1. E. M. Dianov and A. M. Prokhorov, IEEE J. Sel. Top. Quantum Electron. **6,** 1022 (2000).
2. G. M. A. Gad, H. J. Eichler, and A. A. Kaminskii, Opt. Lett. **28,** 426 (2003).
3. S. Spillane, T. Kippenberg, and K. Vahala, Nature **415,** 621 (2002).
4. D. W. Vernooy, V. S. Ilchenko, H. Mabuchi, E. W. Streed, and H. J. Kimble, Opt. Lett. **23,** 247 (1998).
5. S.-X. Qian and R. K. Chang, Phys. Rev. Lett. **56,** 926 (1986).
6. H.-B. Lin and A. J. Campillo, Phys. Rev. Lett. **73,** 2440 (1994).
7. M. Cai, O. Painter, and K. J. Vahala, Phys. Rev. Lett. **85,** 74 (2000).
8. M. L. Gorodetsky and V. S. Ilchenko, J. Opt. Soc. Am. B **16,** 147 (1999).
9. T. J. Kippenberg, S. M. Spillane, and K. J. Vahala, Opt. Lett. **27,** 1669 (2002).
10. H. Haus, *Waves and Fields in Optoelectronics* (Prentice-Hall, Englewood Cliffs, N.J., 1984).
11. D. Braunstein, A. M. Khazanov, G. A. Koganov, and R. Shuker, Phys. Rev. A **53,** 3565 (1996).
12. The relation between g_j and $g_R{}^B$ is given by $g_j = (\lambda_1/\lambda_j)[c^2/(2n^2V_{\text{eff}})]g_R{}^B$. For simplicity the mode volume V_{eff} is assumed to be independent of wavelength.